

Supplement of Atmos. Chem. Phys., 17, 9469–9484, 2017
<https://doi.org/10.5194/acp-17-9469-2017-supplement>
© Author(s) 2017. This work is distributed under
the Creative Commons Attribution 3.0 License.



Supplement of

Simultaneous measurements of new particle formation at 1 s time resolution at a street site and a rooftop site

Yujiao Zhu et al.

Correspondence to: Xiaohong Yao (xhyao@ouc.edu.cn)

The copyright of individual parts of the supplement might differ from the CC BY 3.0 License.

20 **Supporting Text**

FMPS data correction

First step: When the two FMPS operated side-by-side during 12-17 April 2012 for intercomparison, we get the correction factors for one FMPS (following Table S1). In this table, the FMPS which operating simultaneously with a CPC at the street site afterwards was used as the reference to correct the other.

25 **Table S1** Correction factors for one FMPS

D_p	r	D_p	r
8.06	1.294	34	1.222
9.31	1.178	39.2	1.237
10.8	1.134	45.3	1.261
12.4	1.100	52.3	1.292
14.3	1.067	60.4	1.284
16.5	1.051	69.8	1.230
19.1	1.069	80.6	1.200
22.1	1.134	93.1	1.194
25.5	1.189	107.5	1.244
29.4	1.207		

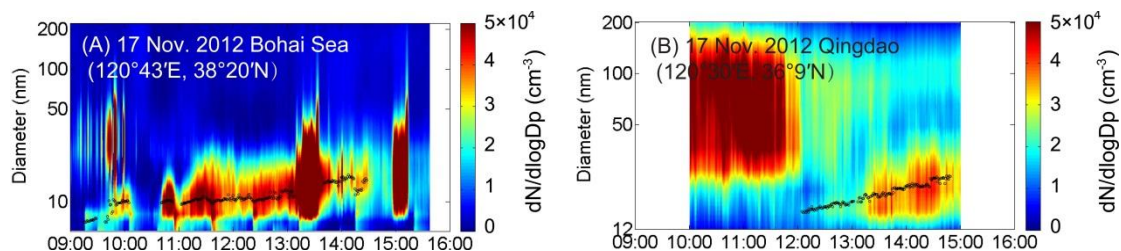
Second step: The FMPS operating simultaneously with a CPC at the street site was then processed the second-step correction proposed by Zimmerman et al. (2015). The ratio of $FMPS_{total}/CPC_{total}$ was calculated to be 1.28.

30 Third step: The calculated ratio of 1.28 and correction method in Zimmerman et al. (2015) was used to correct the FMPS data at the rooftop site.

Evidences of Class II NPF events regarding as regional NPF events

In this study, Class II NPF events lasted for 4-8 hours should be considered as regional NPF events, rather than
35 emission sources or plume events. The reasons were presented as follows:

- 1) As reviewed by Vu et al. (2015), the particle number size distribution (PNSD) of combustion emission source (e.g., traffic emissions, industrial emissions, biomass burning, cooking) characters the typical peak number mode, such as at 30 nm, 50 nm, 70-80 nm, 120-140 nm, et al. When the NPF events in Class II occurred in our study, the nucleation mode particles overwhelmed and those >30nm particle modes were negligible.
 - 2) Similar to Class II NPF events with the particle growth to be undetectable presented in this study, extremely low growth rate of newly formed particles ($\sim 1 \text{ nm h}^{-1}$) in Beijing was also previously reported by Wehner et al. (2004). In our unpublished data, we simultaneously observed Class II NPF events and NPF events with extremely low growth rate at ~ 240 km distance as Figure shown below. In the last three years (data unpublished), we conducted simultaneous observations of NPF events at 100-500 km distance. We obtained six cases based on the simultaneous observations at two locations, i.e., one
45 case featured by Class II NPF vs Class II NPF, four cases featured by Class II NPF vs NPF with an extremely low growth rate, one case featured by Class II NPF vs NPF with “banana shape” particle growth. Class II NPF observed in Bohai Sea, no local combustion sources except vessel emissions characterized by strong > 30 nm particle mode in number concentration spectrum was expected. By considering the six-hours duration of Class II NPF and 0~20 km/hr cursing speed, Class II NPF observed in the marine atmosphere should occur regionally.
 - 3) In this study, the duration period of Class II events lasted for 4-8 hours with the wind speed >4m/s. We strongly believed that they should be considered as regional NPF events.
- 50



55 **To calculate 25% minimum coefficient of variation**

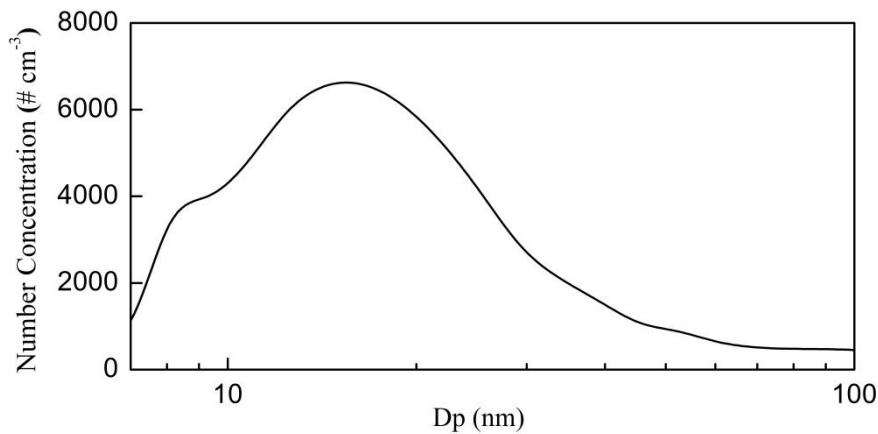
Coefficient of variation (CV) is the ratio of standard deviation to mean for particle number concentration in every 60s. We sort the data sequence in an order from the smallest to the largest, and the minimum 25% values of CV reflect smaller changes of particle number concentration. Large CV values reflect dramatic changes of particle number concentration and are usually caused by turbulence or source emissions (Meng et al., 2015a). In this study, 25% minimum CV was used as an indicator to eliminate the vehicle-caused spikes inside street canyon. For example, in Fig. 5c, all data points on the black solid lines represent the one-minute average number concentration of particles and their CV values in every minute was subject to 25% minimum CV.

Second approach to deduct the contribution of vehicle spikes

The measured number concentrations and size distributions of vehicle particles vary a lot at the street site. Here we considered that particles with the total number concentration larger than 5×10^4 particle cm^{-3} were mainly from the vehicle emissions. During the winter sampling period, we thereby selected eighteen vehicle spikes covering total 20 minutes and plot the averaged vehicle particle size distributions (following figure). In this particle size distribution, $N_{dp}/N_{16.5nm}$ is shown in the following table. Thus we do the calculation as the following equation:

$$N_{dp,deduct} = N_{dp,original} - \frac{N_{dp}}{N_{16.5nm}} \times N_{16.5nm,original}$$

where the $N_{dp,deduct}$ is the number concentration of $D_p(\text{nm})$ particles deducted the vehicle particles, $N_{dp,original}$ is the original number concentration of $D_p(\text{nm})$ particles, $N_{16.5nm,original}$ is the original number concentration of 16.5 nm particles.

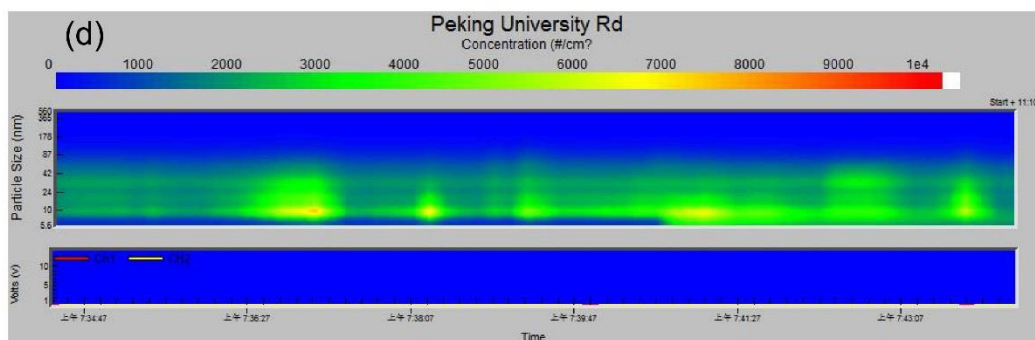
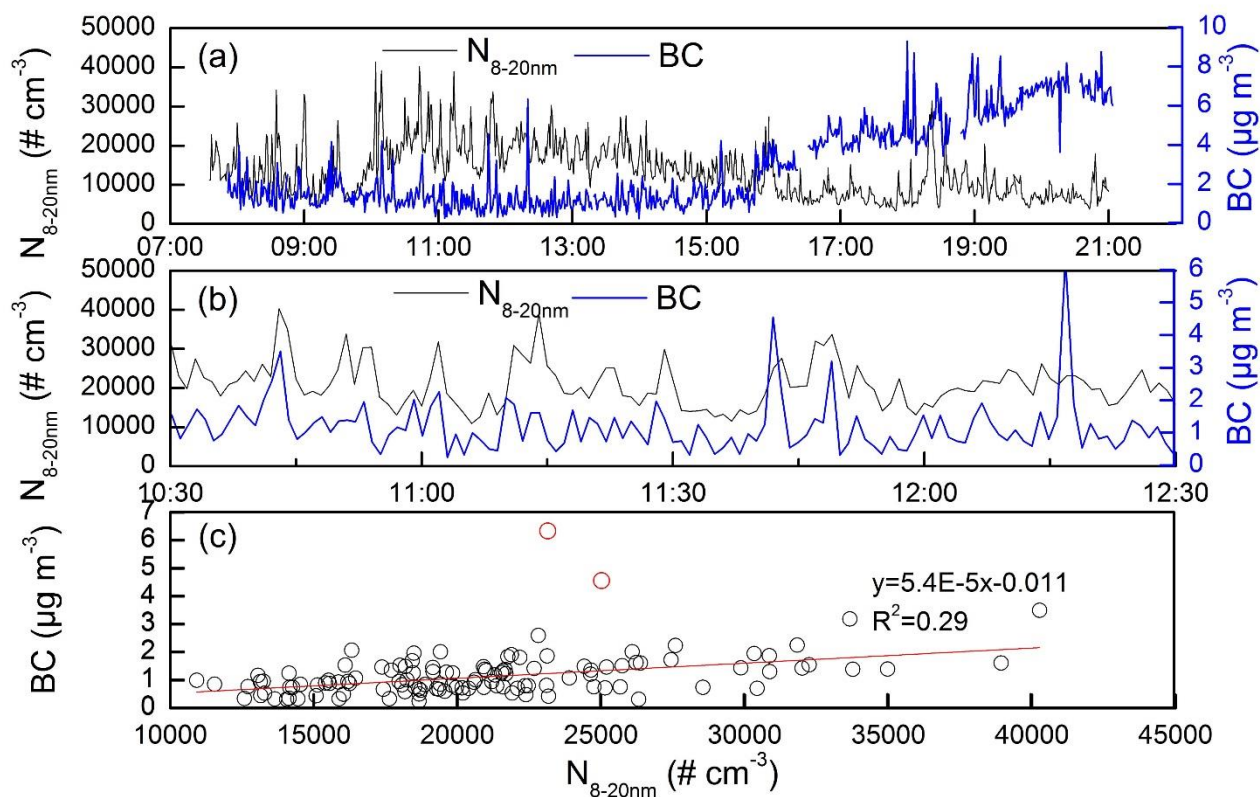


D_p (nm)	$N_{dp}/N_{16.5nm}$	D_p (nm)	$N_{dp}/N_{16.5nm}$
6.04	0.156186	25.5	0.613456
6.98	0.167354	29.4	0.432448
8.06	0.506914	34	0.318763
9.31	0.609134	39.2	0.238996
10.8	0.734096	45.3	0.165393
12.4	0.90152	52.3	0.134049
14.3	0.995841	60.4	0.097849
16.5	1	69.8	0.07806
19.1	0.925529	92.5	0.071186
22.1	0.789295	114.1	0.056596

75 **Using BC data to deduct the contribution of vehicle spikes**

Black carbon (BC) or NO_x were proposed to deduct the contribution of vehicle spikes in literatures (Fruin et al., 2004; Wang et al., 2012). In this study, black carbon (BC) was measured by a portable aethalometer at the street site and BC is a good indicator of traffic emission (Fruin, et al., 2004; Meng et al., 2015a,b). We tried to use BC as an indicator of vehicle emission plumes to deduct primary traffic particles. It does not work because the one-minute time resolution is too low to
80 successfully deduct primary traffic particles. To best of our knowledge, NO_x analyzers are usually set for operating in one-minute time resolution and the data of NO_x may suffer from the same problem. An example is presented to illustrate the problem for using BC to deduct primary traffic particles.

During the entire sampling period on 22 December 2010, BC shows no correlation with the nucleation mode PNC (the following Figure a). During a few short periods, the BC spikes appeared to be visibly consistent with the PNC spikes as
85 shown in Figure b. However, the correlation obtained was much poor, e.g., during the period of 10:30-12:30 (Figure c). This is not surprised because the aethalometer reported the instantaneous value of BC in one minute, but the raw FMPS data showed the vehicle spikes physically occurred in a few seconds (Figure d). Under such poor correlation, the regression equation is invalid to accurately deduct primary traffic particles.



90

Uncertainty analysis of presumption the identical SO_2 at the two sites

The sulfur content in the gasoline and diesel was limited <50 ppm at that years. The measured BC spikes were lower than $5 \mu\text{g m}^{-3}$ during the NPF periods. The maximum contribution of traffic-related SO_2 at the street site was roughly estimated to be 1.3 ppb according to the results in our previous studies (Meng et al., 2015a,b). In the wintertime, the ratio of

95 traffic-derived SO₂ to the observed values was less than 1/4 and the observed values were overwhelmingly contributed by domestic heating. The uncertainty by assuming SO₂ at the street site same as the rooftop site should be minor in the wintertime and it should not affect our conclusion because the formation rates of new particles at the street site were increased by 3-5 times against the rooftop site in the wintertime. In the springtime, the contribution of traffic-related SO₂ might significantly increase the mixing ratio of SO₂ at the street site. However, the reduced NPF was observed at the street
100 site. The possible underestimation of SO₂ at the street site further solidified our analysis results, i.e., a strong scavenge effect at the street site likely existed and caused the reduced NPF.

References:

- Fruin, S. A., Winer, A. M., and Rodes, C. E.: Black carbon concentrations in California vehicles and estimation of in-vehicle diesel exhaust particulate matter exposures, *Atmos. Environ.*, 38, 4123-4133, doi:10.1016/j.atmosenv.2004.04.026, 2004.
- Meng, H., Zhu, Y., Evans, G. J., and Yao, X.: An approach to investigate new particle formation in the vertical direction on the basis of high time-resolution measurements at ground level and sea level, *Atmos. Environ.*, 102, 366-375, doi:10.1016/j.atmosenv.2014.12.016, 2015a.
- 110 Meng, H., Zhu, Y. J., Evans, G., Jeong, C. H., and Yao, X. H.: Roles of SO₂ oxidation in new particle formation events, *J. Environ. Sci.*, 30, 90-101, doi:10.1016/j.jes.2014.12.002, 2015b.
- Vu, T. V., Delgado-Saborit, J. M., and Harrison, R. M.: Review: Particle number size distributions from seven major sources and implications for source apportionment studies, *Atmos. Environ.*, 122, 114-132, doi:10.1016/j.atmosenv.2015.09.027, 2015.
- 115 Wang, X., Westerdahl, D., Hu, J., Wu, Y., Yin, H., Pan, X., and Zhang, K. M.: On-road diesel vehicle emission factors for nitrogen oxides and black carbon in two Chinese cities, *Atmos. Environ.*, 46, 45-55, doi:10.1016/j.atmosenv.2011.10.033, 2012.
- Wehner, B., Wiedensohler, A., Tuch, T. M., Wu, Z. J., Hu, M., Slanina, J., and Kiang, C. S.: Variability of the aerosol number size distribution in Beijing, China: New particle formation, dust storms, and high continental background,
120 *Geophys. Res. Lett.*, 31, doi:10.1029/2004GL021596, 2004.

Zimmerman, N., Jeong, C. H., Wang, J. M., Ramos, M., Wallace, J. S., and Evans, G. J.: A source-independent empirical correction procedure for the fast mobility and engine exhaust particle sizers, *Atmos. Environ.*, 100, 178-184, doi:10.1016/j.atmosenv.2014.10.054, 2015.

125 **Supporting figures and tables**

Fig. S1 Variations of Temperature during sampling days.

Fig. S2 NPF events in Class I at the rooftop site (a: 12 April 2012, b: 13 April 2012, c: 14 April 2012, d: 16 April 2012.

Black dots were the fitted geometric median diameter of new particles (D_{pg}), yellow dots and magenta dots represent the mixing ratios of NO_2+O_3 and SO_2 , respectively, while the values correspond to the right Y Axis).

130 **Fig. S3** Meteorological conditions on 27 April 2012

Fig. S4 Meteorological conditions on 25 April 2012.

Fig. S5 Contour plots, time series of number concentrations and size distributions of atmospheric particles at two sampling sites on 23 Decemebr 2011 (a, b: Contour plots of particle number concentration ($\# \text{ cm}^{-3}$); c: time series of nucleation mode PNC ($N_{8-20\text{nm}}$) and SO_2 mixing ratios at two sampling sites; d: size distributions of $N_{(ts1)}-N_{(ts0)}$ at the street site and $N_{(tr1)}-N_{(tr0)}$

135 on the rooftop).

Fig. S6 Meteorological conditions on 22 December 2011.

Table S1 Correction factors for one FMPS.

Table S2 Characteristics of NPF events at two sites in April 2012 and December 2011.

140

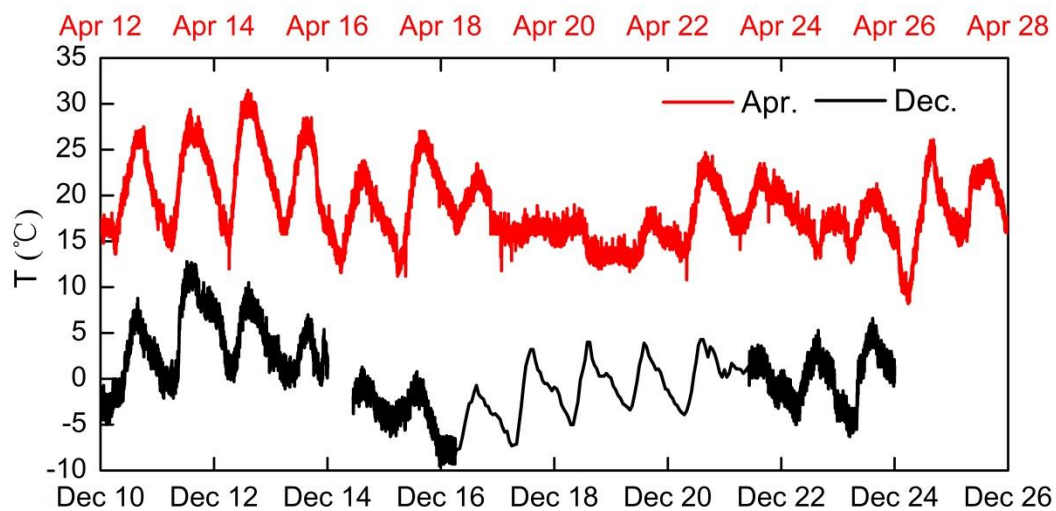
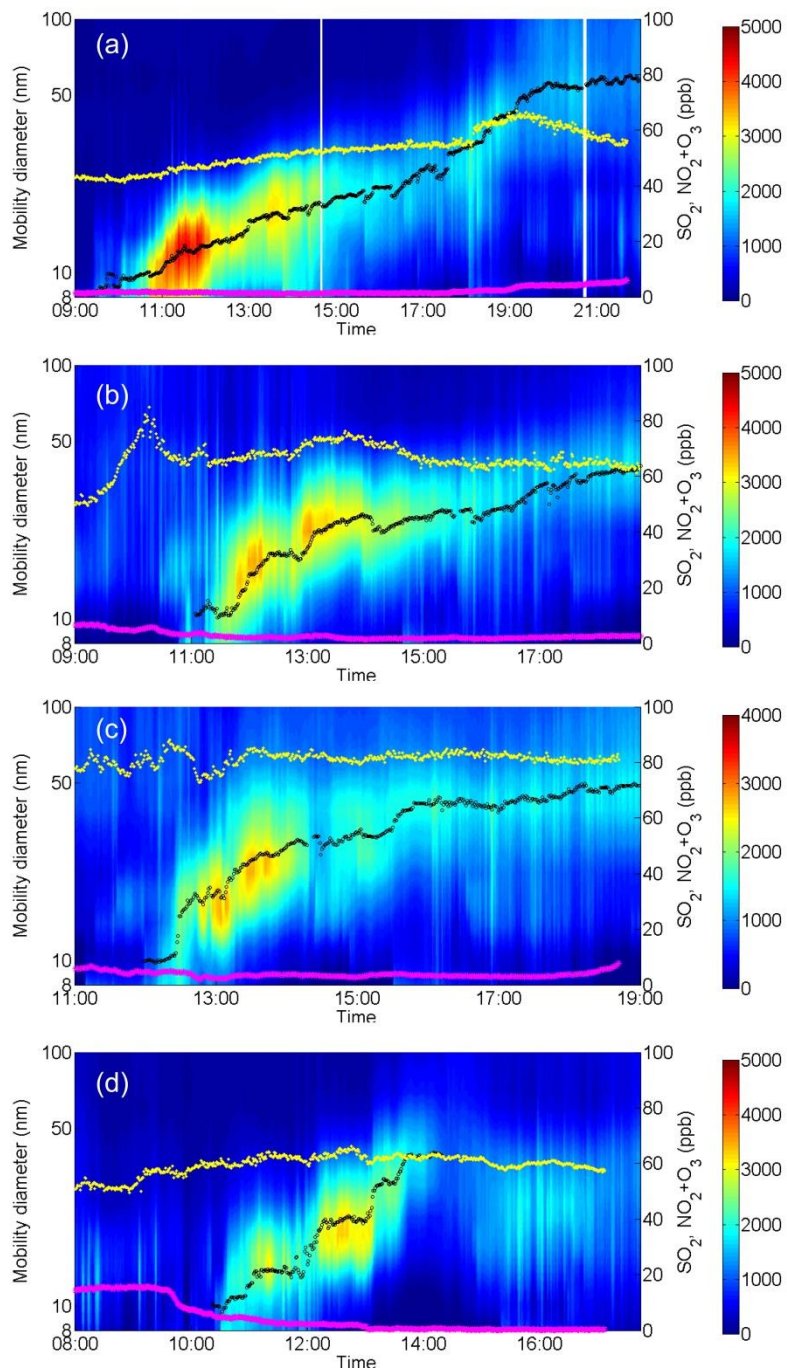
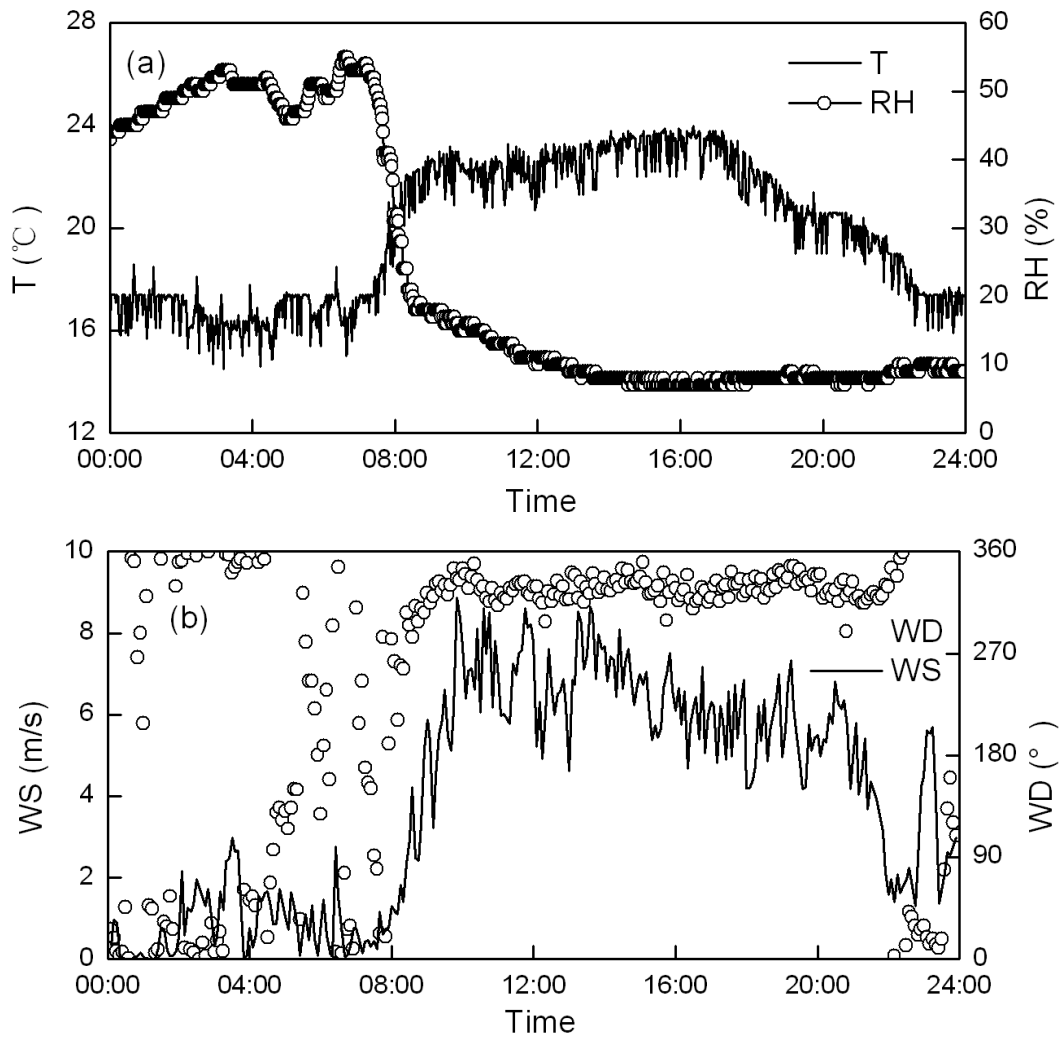


Fig. S1 Variations of Temperature during sampling days.

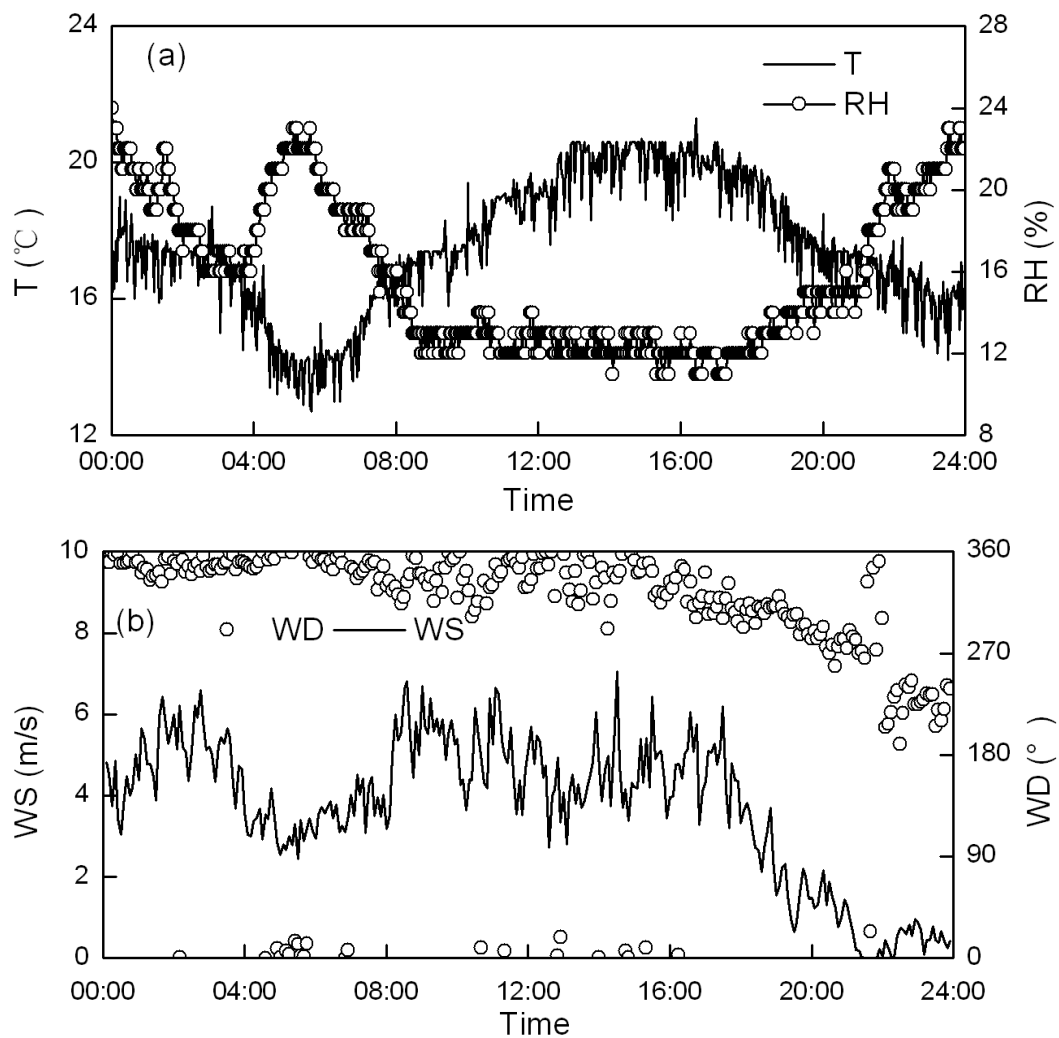


145 **Fig. S2** NPF events in Class I at the rooftop site (a: 12 April 2012, b: 13 April 2012, c: 14 April 2012, d: 16 April 2012. Black dots were the fitted geometric median diameter of new particles (D_{pg}), yellow dots and magenta dots represent the mixing ratios of $\text{NO}_2 + \text{O}_3$ and SO_2 , respectively, while the values correspond to the right Y Axis).



150

Fig. S3 Meteorological conditions on 27 April 2012



155 **Fig. S4** Meteorological conditions on 25 April 2012.

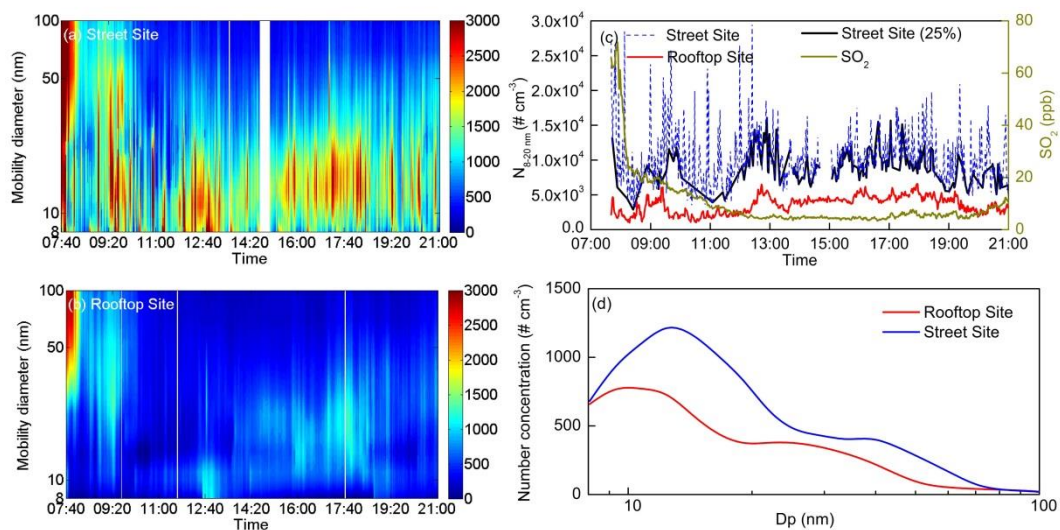
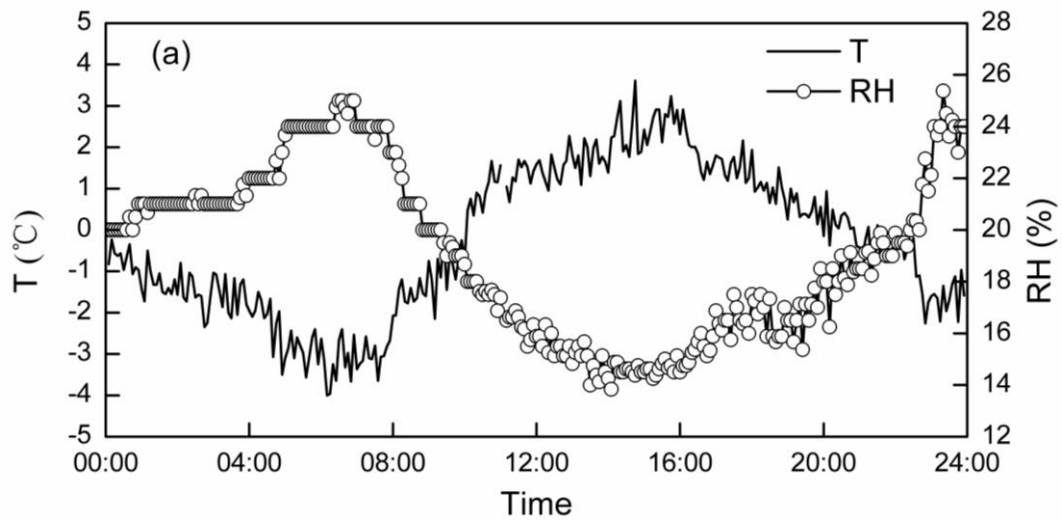


Fig. S5 Contour plots, time series of number concentrations and size distributions of atmospheric particles at two sampling sites on 23 Decemebr 2011 (a, b: Contour plots of particle number concentration ($\# \text{ cm}^{-3}$); c: time series of nucleation mode PNC ($N_{8-20 \text{ nm}}$) and SO_2 mixing ratios at two sampling sites; d: size distributions of $N_{(ts1)}-N_{(ts0)}$ at the street site and $N_{(tr1)}-N_{(tr0)}$ on the rooftop).



165

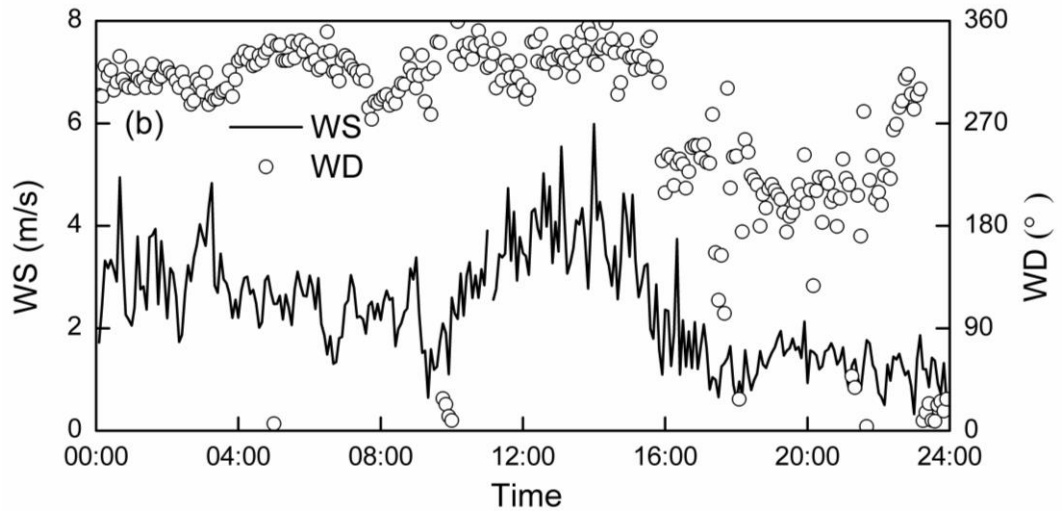


Fig. S6 Meteorological conditions on 22 December 2011.

170

Table S1 Correction factors for one FMPS.

D_p	r	D_p	r
8.06	1.294	34	1.222
9.31	1.178	39.2	1.237
10.8	1.134	45.3	1.261
12.4	1.100	52.3	1.292
14.3	1.067	60.4	1.284
16.5	1.051	69.8	1.230
19.1	1.069	80.6	1.200
22.1	1.134	93.1	1.194
25.5	1.189	107.5	1.244
29.4	1.207		

Table S2 Characteristics of NPF events at two sites in April 2012 and December 2011.

Date	Location	J_8 (particle $\text{cm}^{-3}\text{s}^{-1}$)	GR (nm h^{-1})	CS (10^{-2} s^{-1}) ^a
12 April 2012	Rooftop Site	5	2.2	0.27±0.07
13 April 2012	Rooftop Site	12.2	6	1.4±0.65
14 April 2012	Rooftop Site	9.7	9.3	1.7±0.59
15 April 2012	Rooftop Site	8.4	-	1.3±0.25
16 April 2012	Rooftop Site	8.5	7.9	0.44±0.11
25 April 2012	Rooftop Site	14/49/36/34/1.9*	-	0.16±0.02
	Street Site	13/38/19/17/1.9*	-	0.65±0.23
27 April 2012	Rooftop Site	10.2	-	0.75±0.21
	Street Site	8.1	-	1.2±0.37
10 December 2011	Street Site	5.7	-	2.3±0.51
11 December 2011	Street Site	11	-	8.9±2.5
14 December 2011	Street Site	10.7	-	1.6±0.25
15 December 2011	Street Site	5	-	1.5±0.46
21 December 2011	Rooftop Site	0.9	-	0.45±0.04
	Street Site	4	-	1.3±0.23
22 December 2011	Rooftop Site	1.9	-	0.78±0.17
	Street Site	7.9	-	1.3±0.33
23 December 2011	Rooftop Site	0.8	-	0.98±0.12
	Street Site	4.4	-	1.3±0.23

^a: Condensation sink was averaged 1-h prior to the NPF event.

-: NPF in Class II.

180 *: J_8 of four short-lived NPF events and one regional NPF event.